Cell Reports
Report

Cell PRESS
Open ACCESS

Two Wnts Instruct Topographic Synaptic Innervation in *C. elegans*

Kota Mizumoto[1] and Kang Shen[1,*]
[1]Howard Hughes Medical Institute, Department of Biology, Stanford University, 385 Serra Mall, Stanford, CA 94305, USA
*Correspondence: kangshen@stanford.edu
http://dx.doi.org/10.1016/j.celrep.2013.09.011

SUMMARY

Gradients of topographic cues play essential roles in the organization of sensory systems by guiding axonal growth cones. Little is known about whether there are additional mechanisms for precise topographic mapping of synaptic connections. Whereas the *C. elegans* DA8 and DA9 neurons have similar axonal trajectories, their synapses are positioned in distinct but adjacent domains in the anterior-posterior axis. We found that two Wnts, LIN-44 and EGL-20, are responsible for this spatial organization of synapses. Both Wnts form putative posterior-high, anterior-low gradients. The posteriorly expressed LIN-44 inhibits synapse formation in both DA9 and DA8, and creates a synapse-free domain on both axons via LIN-17/Frizzled. EGL-20, a more anteriorly expressed Wnt, inhibits synapse formation through MIG-1/Frizzled, which is expressed in DA8 but not in DA9. The Wnt-Frizzled specificity and selective Frizzled expression dictate the stereotyped, topographic positioning of synapses between these two neurons.

INTRODUCTION

The developing nervous system encodes spatial information by using topographic map formation, a prevalent organizational principle whereby axonal projections follow a specified arrangement pattern in two-dimensional space. Molecular axon guidance cues, often in the form of local gradients, play instructive roles in topographic map formation (Charron and Tessier-Lavigne, 2005, 2007; Luo and Flanagan, 2007). For instance, the graded expressions of ephrins and their receptors, Ephs, play critical roles in matching the spatial relationship of the cell bodies in the retina with their axon termination zone in the target area, the superior colliculus (or optic tectum) (McLaughlin and O'Leary, 2005). Similarly, semaphorins and their receptors, plexins and neuropilins, are required for topographic map formation in the olfactory system (Imai et al., 2009; Komiyama et al., 2007; Sweeney et al., 2011).

Wnt signaling, which is involved in many developmental processes, including stem cell maintenance and differentiation, also plays critical roles in axon targeting during topographic map formation (Logan and Nusse, 2004). Schmitt et al. (2006) reported that Wnt3 forms a gradient in a medial-lateral axis in both the chick optic tectum and mouse superior colliculus. Retinal ganglion cells express a Wnt receptor, Ryk, in a ventral-high, dorsal-low gradient. Wnt3 repels axons from Ryk-expressing neurons, thereby establishing the projection map (Schmitt et al., 2006). Similarly, DWnt4, which is expressed in the ventral lamina, is required for the dorsoventral projections of the photoreceptor neurons in the fly eye (Sato et al., 2006).

Reconstruction of the *Caenorhabditis elegans* nervous system by electron microscopy revealed not only topographic arrangement of axons but also precise topographic organization of synapses (White et al., 1976). The majority of the motoneurons place their en passant synapses according to their cell body position. Several recent papers have shown that the precise control of synapse position in this system is mediated by signaling molecules that were previously known to direct axon targeting (Klassen and Shen, 2007; Mizumoto and Shen, 2013; Poon et al., 2008). For example, we recently reported that semaphorin/plexin signaling mediates the mutual exclusion of synaptic regions between contacting axons, leading to the generation of tiled synaptic innervation in *C. elegans* (Mizumoto and Shen, 2013). The ability of the semaphorin/plexin/neuropilin signaling pathway to precisely regulate synaptic connectivity was also shown in several vertebrate systems (Ding et al., 2012; Pecho-Vrieseling et al., 2009; Tran et al., 2009).

Wnt signaling has been reported to inhibit synapse formation in *C. elegans* and *Drosophila* motoneurons. This inhibitory activity is used both to direct precise subcellular synapse localization and to specify synaptic connectivity (Inaki et al., 2007; Klassen and Shen, 2007; Park and Shen, 2012). Wnt has also been shown to promote synaptogenesis in several systems. In the mouse cerebellum, Wnt7a regulates remodeling of the axon terminal and promotes maturation of the synaptic complexes. At the *Drosophila* neuromuscular junction, Wnts regulate postsynaptic receptor localization, synaptic structure differentiation, and synaptic plasticity (Budnik and Salinas, 2011; Hall et al., 2000; Packard et al., 2002). In hippocampal neurons, the activation of the canonical Wnts increases presynaptic inputs, whereas the noncanonical Wnt5a decreases the number of presynaptic terminals, suggesting that different Wnt signaling pathways could have opposite effects on synapse formation (Davis et al., 2008).

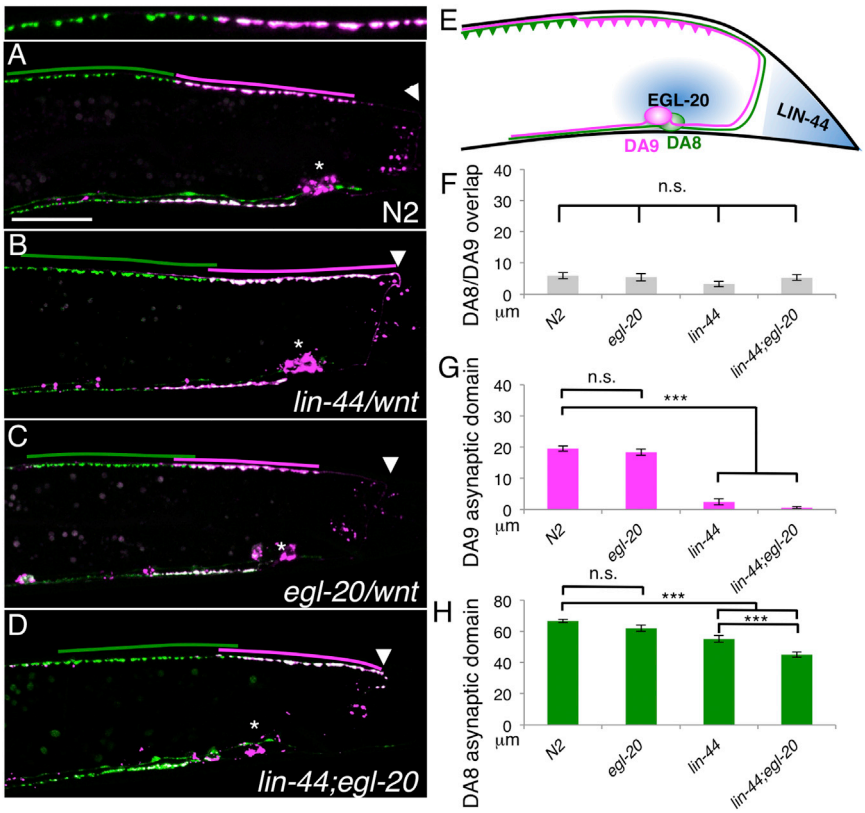

Figure 1. Synaptic Tiling Is Maintained in *wnt* Mutants

(A–D) Representative images of DA8/DA9 synaptic patterns in N2 (wild-type) (A), *lin-44* (B), *egl-20* (C), and *lin-44;egl-20* (D) animals. Asterisks represent the positions of the DA8/DA9 cell bodies. Arrowheads indicate the position of the DA9 commissure. Scale bar: 20 μm.

(E) Schematic representation of DA8 and DA9 projection patterns and Wnt gradients.

(F) Quantification of the overlap between the DA8 and DA9 synaptic domains. DA8/DA9 overlap is defined as the distance between the most anterior DA9 synapse and the most posterior DA8 synapse.

(G) Quantification of the DA9 asynaptic domains. The DA9 asynaptic domain is defined as the distance between the most posterior DA9 synapse and the DA9 commissure.

(H) Quantification of the DA8 asynaptic domains. The DA8 asynaptic domain is defined as the distance between the most posterior DA8 synapse and the DA9 commissure. Since the DA8 commissure is located in the same place as the DA9 commissure in terms of the A-P axis, we used the position of the DA9 commissure, which is easier to identify. Error bars represent SEM. n.s., not significant; ***$p < 0.001$ (ANOVA/Tukey's honestly significant difference [HSD] test).

See also Figure S1.

Synapse topographic maps are also found in vertebrates. In the mouse hippocampus, CA3 neurons form a small number of en passant terminal arbors (synaptic complexes) on their axons. The position of the synaptic complexes made by each cell is preordained by its cell body position, a phenomenon that is dependent on EphA4 (Galimberti et al., 2010). It is likely that many more examples of synaptic topographic maps will be discovered as more sophisticated labeling tools are developed. The exact mechanisms that create synaptic topographic maps, however, remain unclear. How do neurons of the same class place their synapses in stereotyped positions with regard to each other?

Here, by analyzing the relative synaptic positions of different neurons within the same class in *C. elegans*, we found that two Wnt gradients play a critical role in topographic synaptic pattern formation along the anterior-posterior (A-P) axis in vivo. Whereas both DA8 and DA9 motoneurons respond to the more posterior Wnt gradient, which is composed of LIN-44, DA8 neuron is more sensitive than DA9 to the more anteriorly expressed EGL-20/Wnt. This differential sensitivity is accomplished by the preferential expression of the MIG-1/Frizzled receptor in DA8. Loss- and gain-of-function experiments revealed that the EGL-20-MIG-1 signaling pathway is responsible for placing DA8 synapses in an anterior location. We propose that the combination of Wnts and selective Frizzled expression functions alongside the previously described axon-axon interactions to establish the stereotyped synaptic pattern of DA motoneurons in vivo.

RESULTS

Wnt Signaling Functions in Parallel with Synaptic Tiling Mechanisms to Determine Synaptic Topography

We have previously shown that LIN-44/Wnt, which is secreted from the hypodermal cells in the tail, prevents synapses from forming in the most posterior dorsal axonal segment of DA9, leaving the DA9 posterior axon "asynaptic" (Herman et al., 1995; Klassen and Shen, 2007; Figures 1A and 1E). In addition, EGL-20/Wnt, which is secreted from cells around the hindgut, resulting in a posterior-high, anterior-low gradient (Coudreuse et al., 2006), inhibits synapses from forming in the commissure of DA9 axon in the *lin-44* mutant background (Klassen and Shen, 2007). In mutants lacking both of these Wnts, presynaptic puncta accumulate in the posterior part of the dorsal axon and in the commissure of the DA9 neuron. It is not known, however, whether LIN-44 and EGL-20 affect the localization of synapses in other DA neurons in the area. This is an especially relevant question with regard to the DA8 neuron, whose cell body position and axonal trajectory are very similar to those of DA9.

In order to visualize the synapses in both DA8 and DA9, we created a stable transgenic strain that expressed the GFP::RAB-3 synaptic vesicle marker in all DA neurons (DA1–DA9) and mCherry::RAB-3 only in the DA9 neuron. As a result, the DA8 (and other anterior DA) synapses were labeled with green fluorescence and the DA9 synapses were labeled with both green and red fluorescence (pseudocolored in magenta). In wild-type animals, although the DA8 and DA9 axons both

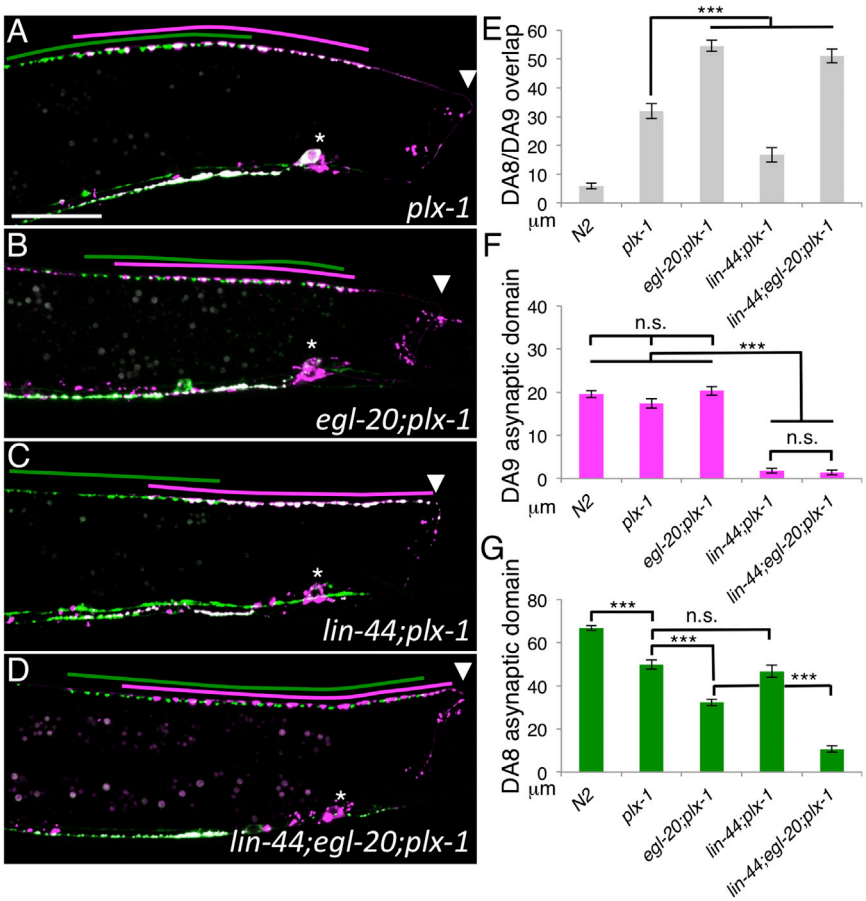

Figure 2. Distinct Response of the DA8 and DA9 Neurons to LIN-44 and EGL-20

(A–D) Representative images of DA8/DA9 synaptic patterns in *plx-1* (A), *egl-20; plx-1* (B), *lin-44; plx-1* (C), and *lin-44; egl-20; plx-1* (D) mutant animals. Asterisks represent the positions of DA8/DA9 cell bodies. Arrowheads indicate the position of the DA9 commissure. Scale bar: 20 μm.

(E) Quantification of the overlap between the DA8 and DA9 synaptic domains.

(F) Quantification of the DA9 asynaptic domains.

(G) Quantification of the DA8 asynaptic domains. Error bars represent SEM. n.s., not significant; ***$p < 0.001$ (ANOVA/Tukey-HSD).

See also Figures S2–S4.

extend along roughly half of the animal and overlap significantly with each other, they form tiled synaptic innervations by restricting their synapses to two adjacent, nonoverlapping axonal domains in the dorsal nerve cord (Figures 1A and 1E). We have shown that interaxonal interaction between DA8 and DA9, mediated by a transmembrane semaphorin (*smp-1*) and plexin (*plx-1*), generates the tiled synaptic domains (Mizumoto and Shen, 2013). In *smp-1* or *plx-1* mutants, the DA8 and DA9 synapse domains expand and overlap with each other (Figure 2A; Mizumoto and Shen, 2013).

The stereotyped synaptic pattern comprised of the DA8 and DA9 synapses is characterized not only by the tiled synaptic domains but also by the invariable relative position of those domains from the two cells: the DA8 synaptic domain is always anterior to the DA9 synaptic domain. This relative position was present even in the *plx-1* or *smp-1* mutants (Figure 2A and Figure S2A available online), suggesting that additional mechanisms are responsible for the positional bias of DA8 and DA9 synapses. To explore these mechanisms, we examined the position of DA8 and DA9 synapses in Wnt mutants. In *lin-44* mutants, as we reported previously (Klassen and Shen, 2007), the DA9 synaptic domain was shifted posteriorly. We found that the DA8 synaptic domain was also displaced posteriorly but still tiled with the DA9 synaptic domain (Figures 1B, 1F, and 1G), resulting in a posterior shift of the DA8/DA9 synaptic tiling border (Figure 1H). In *egl-20* mutants, the position of both the DA8 and DA9 synaptic domains, as well as that of the synaptic tiling border, remained unaffected (Figure 1C), likely because the plexin-mediated synaptic tiling mechanism masked the effect of EGL-20 on DA8 (see below). However, *egl-20* enhanced the *lin-44* mutant phenotype: in *lin-44; egl-20* double mutants, the synaptic tiling border was further shifted posteriorly compared with *lin-44* single mutants (Figures 1D and 1H), suggesting that EGL-20 and LIN-44 cooperatively regulate the position of both DA8 and DA9 synaptic domains. We did not observe a synaptic tiling defect in the *lin-44; egl-20* double mutants, which suggests that the synaptic tiling mechanism mediated by contact-dependent plexin signaling acts in parallel with the Wnts to position synapses. Consistently, PLX-1 is localized at the synaptic tiling border and enriched at the anterior asynaptic domain of the DA9 axon in both wild-type and *lin-44; egl-20* mutant animals (Figure S1; Mizumoto and Shen, 2013).

The DA8 Neuron Is More Sensitive to the Anterior Wnt EGL-20 than the DA9 Neuron

Because synaptic tiling indirectly promotes proper synapse positioning by instructing relative synapse localization, we further dissected the role of Wnts in positioning the DA synapses by using the *plx-1* mutation to disable synaptic tiling between the DA8 and DA9 synapses. We assessed the positions of the DA8 and DA9 synaptic domains with regard to two different parameters. First, the length of the asynaptic domain (defined as the distance between the posterior-most synapse to the axon turning point in the dorsal nerve cord) is a measure of the absolute position of the DA8 and DA9 synaptic domains in the A-P axis. Second, the overlap between the DA8 and DA9 synaptic domains reflects the position of the synaptic domains relative to each other. In *egl-20; plx-1* double mutants, the DA8 and DA9 synaptic domains displayed a much greater degree of overlap than in *plx-1* single mutants, and they almost completely overlapped with each other (Figures 2B and 2E). This phenotype

was caused by the posterior shift of the DA8 synaptic domain, as the DA8 asynaptic domain length was significantly shorter than *plx-1* single mutants, whereas the DA9 asynaptic domain was unaffected (Figures 2F and 2G). This result suggests that EGL-20, which is expressed by a group of cells near the anus, instructs the placement of DA8 synapses anterior to those of DA9. In *lin-44; plx-1* mutants, the DA9 synaptic domain is shifted to the most posterior dorsal axonal region. On the other hand, the absolute position of the DA8 synaptic domain, as determined by the length of DA8 asynaptic domain, was similar to that in the *plx-1* single mutants (Figures 2C and 2G). This result suggests that the DA9 synapses are strongly inhibited by LIN-44, but the DA8 synapses are not. Consistent with this model, the overlap between the DA8 and DA9 synaptic domains was shortened in *lin-44; plx-1* mutants due to the selective posterior shift of the DA9, but not the DA8, domain (Figure 2E).

Interestingly, in *egl-20; plx-1* mutants, the DA8 synapses were still absent from the most posterior dorsal axon, where LIN-44 inhibits DA9 synapse formation (Figure 2B). Therefore, it is possible that DA8 also senses LIN-44 in addition to EGL-20. Consistent with this idea, in *lin-44; egl-20; plx-1* triple mutants, both the DA8 and DA9 synaptic domains were shifted to the most posterior dorsal axonal region. These data suggest that LIN-44 inhibits synapse formation in both DA8 and DA9, whereas EGL-20 predominantly affects DA8 (Figure 2D). The enhancement of synaptic domain mislocalization between *plx-1* and the Wnt genes also indicates that Wnts and synaptic tiling mechanisms function in parallel to control synaptic localization. We consistently observed the same enhancement effects of the Wnt mutations when we used a *smp-1; smp-2* double-mutant background to disable the synaptic tiling mechanisms (Figure S2).

The higher sensitivity of DA8 to EGL-20 could be due to the *egl-20* coding sequence or a posttranslational modification of this Wnt, which is specific to endogenous EGL-20-producing cells (Harterink and Korswagen, 2012). To distinguish between these two possibilities, we ectopically expressed EGL-20 under the *lin-44* promoter, which is expressed in the posterior-most tail hypodermal cells, in the *lin-44; egl-20; plx-1* triple mutant (Figure S3A). In this genetic background, DA8 synapses were anteriorly displaced, whereas DA9 synapses remained unchanged (Figures S3D, S3F, and S3H). On the other hand, expression of LIN-44 from the *egl-20* promoter in the *lin-44; egl-20; plx-1* triple mutant caused both DA8 and DA9 synaptic domains to shift anteriorly, further demonstrating that LIN-44 inhibits both DA8 and DA9 synapses, whereas EGL-20 specifically inhibits DA8 synapses (Figures S3C, S3G, and S3I). As a control, expression of LIN-44 cDNA under its endogenous promoter shifted both DA8 and DA9 synapses (Figures S3B, S3F, and S3H). Similarly, expression of EGL-20 cDNA under the *egl-20* promoter shifted DA8 synapses, but not DA9 synapses (Figures S3E, S3G, and S3I). Taken together, these results argue strongly that the differential effect of LIN-44 and EGL-20 on DA8 and DA9 is not caused by Wnt-producing cells.

To further determine whether Wnts play instructive or permissive roles in synapse patterning, we ectopically expressed LIN-44 and EGL-20 from pharynx (*myo-2* promoter) and vulval precursor (*egl-17* promoter; Figure S3A) cells. Expression of EGL-20 from pharynx cells has been shown to rescue Q cell migration defects, in which EGL-20 acts as a permissive cue (Whangbo and Kenyon, 1999). We found that neither of the Wnts expressed in the anterior cells showed any rescuing effects on the DA8 or DA9 synaptic phenotype, suggesting that Wnts function as instructive cues in patterning synapses (Figures 3F–3I).

MIG-1/Frizzled Is an EGL-20/Wnt Receptor in the DA8 Neuron

We next searched for the mechanisms underlying the high sensitivity of DA8 to EGL-20 compared with DA9. It has been shown that various Wnt receptors have different binding affinities for each Wnt homolog (Kikuchi et al., 2009). There are three major EGL-20 receptors in *C. elegans*: LIN-17 (Frizzled), MIG-1 (Frizzled), and CAM-1 (receptor tyrosine kinase; see below for the *lin-17* mutant phenotype) (Eisenmann, 2005). We found that the DA8 and DA9 synapse positions in *mig-1* and *cam-1* single mutants, as well as in a *mig-1; cam-1* double mutant, were indistinguishable from those in the wild-type (Figures 3A and 3F–3H; data not shown), which is consistent with the observation that the synaptic tiling mechanism masked the effect of EGL-20 on DA8 (Figure 1C). We then tested *mig-1; plx-1* and *cam-1; plx-1* double mutants and found that *mig-1; plx-1*, but not *cam-1; plx-1*, phenocopied the *egl-20; plx-1* strain (Figure 3B; data not shown). In *mig-1; plx-1* double mutants, the DA8 synaptic domain shifted posteriorly and completely overlapped with the DA9 synaptic domain, suggesting that MIG-1 is required for EGL-20 to affect the DA8 synapse position (Figures 3B and 3F–3H). Consistent with this hypothesis, the *egl-20; mig-1; plx-1* triple-mutant strain did not enhance the mislocalization of synapses in either the *mig-1;plx-1* or *egl-20; plx-1* double mutants, suggesting that *egl-20* and *mig-1* act in the same signaling pathway to inhibit DA8 synapse formation (Figures 3F–3H). Therefore, MIG-1/Frizzled likely functions as the EGL-20 receptor in the DA8 neuron.

We next examined the expression pattern of MIG-1. The 3.9 kb genomic fragment upstream of the *mig-1* open reading frame was used to drive membrane-tethered GFP (myr-GFP) expression and injected with a DA9 mCherry marker. Consistent with the genetic data, we found that *Pmig-1::gfp* was expressed in DA8 but was undetectable in DA9 (Figure 3C), suggesting that the selective expression of *mig-1* in DA8 renders the latter sensitive to EGL-20. To test whether MIG-1 is sufficient to cause anterior synapse displacement, we expressed MIG-1 cDNA ectopically in the DA9 neuron in the *plx-1* mutant. Due to the high copy number of the transgene, it is likely that the transgenic animals had a higher level of MIG-1 in DA9 compared with DA8. Therefore, we might expect DA9 to become even more sensitive to EGL-20 than DA8. Indeed, in this genetic background, we found that DA9 synapses were localized anterior to DA8 synapses (59.8%, n = 184; Figure 3D), further supporting the sufficiency of MIG-1 for creating the synaptic position in DA8. This effect of ectopic MIG-1 overexpression was dependent on EGL-20, as *egl-20* mutation suppressed the MIG-1 overexpression phenotype (0.87%, n = 115; Figure 3E). Taken together, our results indicate that MIG-1/Frizzled, which is expressed in DA8 (but not in DA9), is an EGL-20/Wnt receptor that inhibits synapse

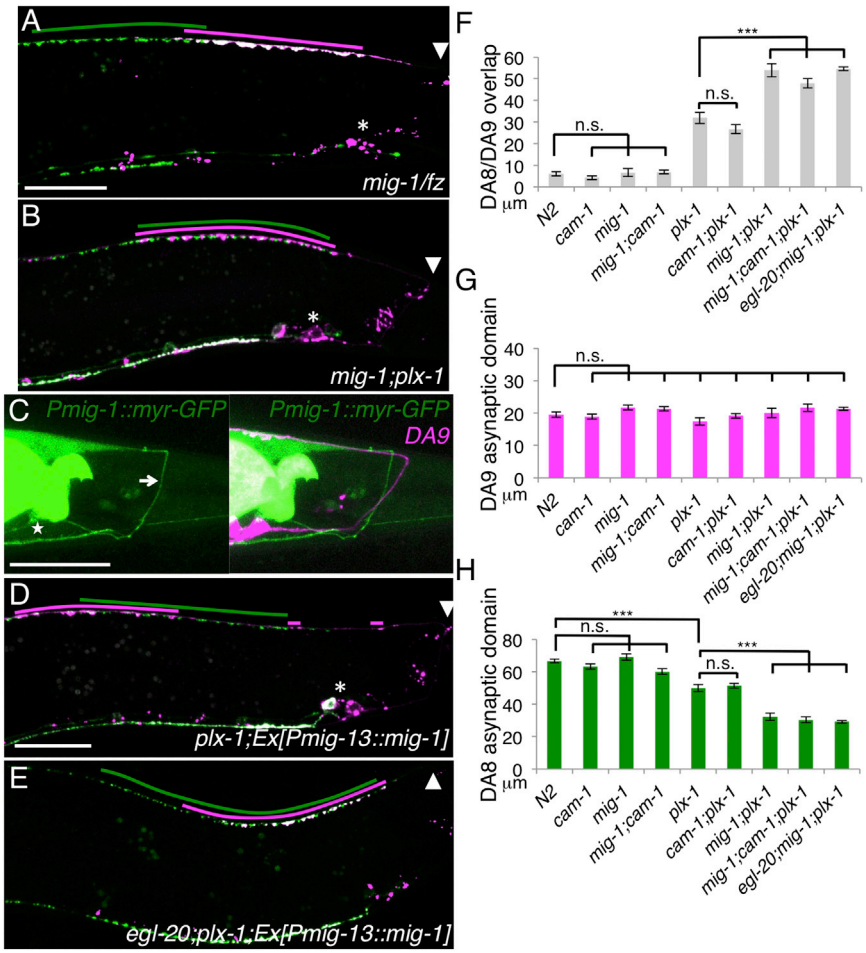

Figure 3. MIG-1/Frizzled Is an EGL-20 Receptor in the DA8 Neuron

(A and B) Representative images of DA8/DA9 synaptic patterns in *mig-1* (A) and *mig-1; plx-1* (B) mutant animals.

(C) Specific expression of the transcriptional reporter *Pmig-1::myr-gfp* in the DA8 neuron. A merged image with the DA9 marker (*Pmig-13::myr-mcherry*) is shown in the right panel. The DA8 cell body and commissure are indicated by a star and arrow, respectively.

(D) Representative image of DA8/DA9 synaptic patterns in the *plx-1* mutant overexpressing *mig-1* in the DA9 neuron. Asterisks represent the positions of DA8/DA9 cell bodies.

(E) Representative image of DA8/DA9 synaptic patterns in *egl-20; plx-1* mutant animals overexpressing *mig-1* in the DA9 neuron. Arrowheads indicate the position of the DA9 commissure. Scale bar: 20 μm.

(F) Quantification of the overlap between the DA8 and DA9 synaptic domains.

(G) Quantification of the DA9 asynaptic domains.

(H) Quantification of the DA8 asynaptic domains. Error bars represent SEM. n.s., not significant; ***$p < 0.001$ (ANOVA/Tukey-HSD).

See also Figure S4.

formation. This difference in EGL-20 sensitivity between the DA8 and DA9 neurons is key in positioning the DA8 synaptic domain anterior to that of DA9 (Figure S4).

LIN-17/Frizzled Is Required in Both DA8 and DA9 to Receive Wnt Signals

We have shown previously that LIN-17 (Frizzled) is required cell autonomously in DA9 to respond to LIN-44 and EGL-20 (Klassen and Shen, 2007). Because DA8 synapses are absent from the most posterior axonal region in *plx-1; egl-20* or *plx-1; mig-1* double-mutant animals, it is possible that LIN-17 is also required in DA8. Indeed, in *lin-17; plx-1* double mutants, both the DA8 and DA9 synaptic domains were shifted to the most posterior dorsal axon (Figures 4A and 4C–4E). This synaptic domain shift was similar to that observed in the *lin-44; egl-20; plx-1* triple mutant, suggesting that the LIN-17 receptor is necessary to mediate LIN-44 and EGL-20 function in both neurons. To confirm that LIN-17 is required in both DA8 and DA9 to respond to Wnts, we expressed LIN-17 cDNA in both DA8 and DA9 using the *unc-4c* promoter in the *lin-17; plx-1* strain. As expected, we found that both the DA8 and DA9 synaptic domains were shifted anteriorly, whereas expression of LIN-17 in other dorsal motoneurons (DB neurons) from the *unc-129* promoter had no effect on the DA8/DA9 synaptic patterns (Figures 4B–4E). Consistent with the model in which LIN-17 is required to sense both EGL-20 and LIN-44 in DA8, the DA8 synaptic domain was shifted more anteriorly than that of DA9 (Figures 4B, 4D, and 4E). Taking these results together, we conclude that LIN-17 is required in both DA8 and DA9 to sense both the EGL-20 and LIN-44 Wnts (Figure S4).

Our previous study (Klassen and Shen, 2007) showed that LIN-17 localizes to puncta along the posterior asynaptic region of DA9 in a *lin-44*-dependent manner, indicating that LIN-44 not only activates LIN-17 but also restricts its subcellular localization. We next examined the subcellular localization of MIG-1. Due to the lack of a DA8-specific promoter and the fact that ectopic MIG-1 expression in DA9 seems to function in the same manner as endogenous MIG-1 in DA8, we examined MIG-1 subcellular localization by expressing MIG-1::GFP in DA9. We found that MIG-1::GFP exhibited a punctate staining pattern in the posterior dorsal axon, the dendrite, and the cell body, where the EGL-20 concentration is high (Figure 4F). The subcellularly restricted MIG-1::GFP puncta at the dorsal axonal region was completely dependent on EGL-20: in the *egl-20* mutant background, MIG-1::GFP exhibited diffuse localization throughout the axon (Figure 4G). On the other hand, the MIG-1::GFP puncta were not affected by loss of *lin-44* function (Figure 4H). Therefore, EGL-20 not only activates MIG-1 but also patterns its subcellular localization.

Interestingly, in contrast to MIG-1, the LIN-17 subcellular localization pattern was not obviously affected by the *egl-20*

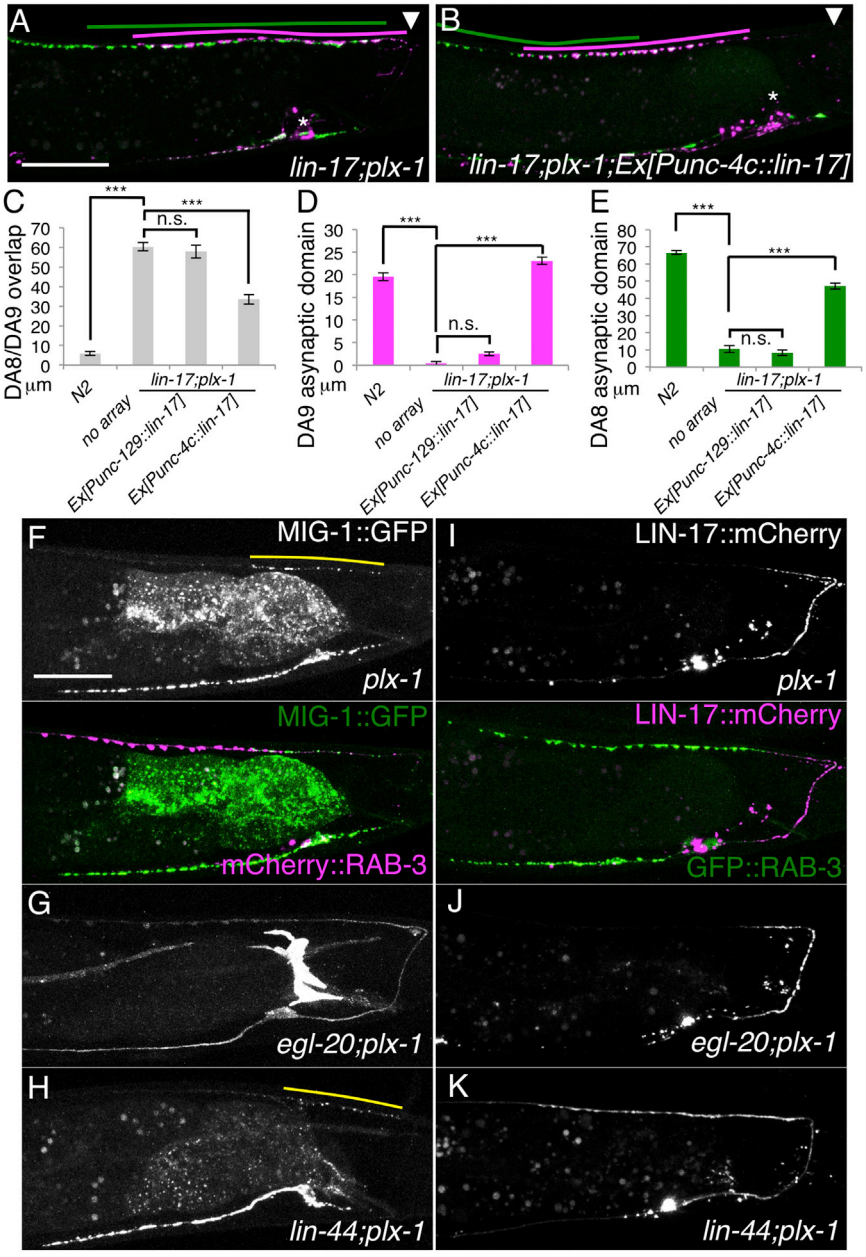

Figure 4. *lin-17* Is Required in Both the DA8 and DA9 Neurons

(A) Representative image of DA8/DA9 synaptic patterns in the *lin-17; plx-1* double mutant.

(B) Representative image of DA8/DA9 synaptic patterns in a *lin-17; plx-1* animal expressing *Punc-4c::lin-17*. Asterisks represent the positions of the DA8/DA9 cell bodies. Arrowheads indicate the position of the DA9 commissure.

(C) Quantification of the overlap between the DA8 and DA9 synaptic domains.

(D) Quantification of the DA9 asynaptic domains.

(E) Quantification of the DA8 asynaptic domains. Error bars represent SEM. n.s., not significant; ***$p < 0.001$ (ANOVA/Tukey-HSD).

(F) Representative image of MIG-1::GFP localization in the DA9 neuron (upper panel). MIG-1::GFP was coexpressed with mCherry::RAB-3 (lower panel).

(G and H) MIG-1::GFP localization in *egl-20* (G) and *lin-44* (H) mutant animals. Yellow lines represent MIG-1::GFP puncta at the dorsal axon.

(I) Representative image of LIN-17::mCherry localization in the DA9 neuron (upper panel). LIN-17::mCherry was merged with GFP::RAB-3 (lower panel).

(J and K) LIN-17-1::mCherry localization in *egl-20* (J) and *lin-44* (K) mutants. Scale bar: 20 μm.

See also Figure S4.

mutation, but it was completely dependent on *lin-44* (Figures 4I–4K). Hence, the Wnt-receptor specificity might help to localize Frizzled in different places to create "synapse-free" zones. Based on these results, we concluded that two Wnts instruct the topographic synaptic pattern by inhibiting synapses in particular subcellular domains (Figure S4).

DISCUSSION

Wnt signaling plays a role in multiple processes during neural circuit development, including axon guidance, polarity establishment, axon regeneration, and synaptic specificity (Park and Shen, 2012). In *Drosophila*, expression of Wnt4 in the M13 muscle cell is required to prevent the motoneurons that innervate the M12 muscle cell from forming ectopic synapses onto M13, suggesting that Wnt4 inhibits synapse formation and helps selective synaptic choice (Inaki et al., 2007). In *C. elegans*, Wnt signaling is involved in many aspects of development involving A-P polarity, such as asymmetric cell division, cell migration, axon/dendrite polarity, and neurite outgrowth (Goldstein et al., 2006; Hilliard and Bargmann, 2006; Kirszenblat et al., 2011; Pan et al., 2006; Sawa, 2012; Silhankova and Korswagen, 2007). Our study revealed that two neurons from a single neuron class form their synaptic domains at distinct regions by differentially responding to two Wnt gradients.

Alterations in Wnt signaling dramatically affected the DA8 and DA9 synaptic patterns in the *plx-1* mutant background. The additive synapse mislocalization phenotype between the *wnt* mutants and the *plx-1* mutant argues strongly that these two pathways act in parallel to pattern synapses. Interestingly, both PLX-1 signaling and the two Wnts restrict synapse formation, setting boundaries for synaptic domains. These results highlight the importance of inhibitory cues in regulating synaptic patterns in vivo. Although the action of EGL-20 and LIN-44, combined with the synaptic tiling pathway, can largely explain the position of the DA8 and DA9 synapses, we rarely observed flipped or

randomized synaptic patterns between the DA8 and DA9 neurons in *wnt* or *frizzled* mutants, suggesting that there are additional mechanisms that determine the position of DA8 and DA9 synapses. One possible mechanism is the developmental timing of these two neurons: either DA8 or DA9 could form synapses first, obliging the remaining neuron's synaptic domain to form in the remaining synapse-free space along the nerve cord. This possibility remains to be tested.

In the DA8 neuron, we found that the posterior displacement of DA8 synapses in the *lin-17; plx-1* double mutant was as strong as that in the *lin-44; egl-20; plx-1* triple mutant, suggesting that in addition to MIG-1/Frizzled, LIN-17/Frizzled is also required to sense EGL-20. We previously reported that *egl-20* significantly enhances *lin-44* synapse displacement in the DA9 neuron, even though we do not detect expression of *mig-1/frizzled* in DA9 (Klassen and Shen, 2007). There are also several reports that LIN-17 acts as a receptor for EGL-20 (Eisenmann, 2005). Frizzled receptors are reported to form homo- or hetero-oligomers (Kaykas et al., 2004). Therefore, it is possible that the DA8 neuron utilizes a MIG-1/LIN-17 heteromultimer to gain higher sensitivity to EGL-20 than the LIN-17 homomultimers in the DA9 neuron. The punctate MIG-1 localization is completely dependent on EGL-20, but not on LIN-44. On the other hand, the LIN-17 localization is more affected by LIN-44 than EGL-20, which suggests Wnt-receptor specificity.

Synaptic tiling and synapse topographic maps have not been extensively described outside of *C. elegans*, likely due to the insufficient resolution of the current labeling tools. However, in one study, Galimberti et al. (2010) observed a synaptic topographic map in a vertebrate system. They reported that in the mouse hippocampus, each granular neuron forms a few large, en passant presynaptic specializations (terminal arborizations [TAs]) in the CA3 region. The positions of the TAs exhibit a striking colinear topographic relationship to the positions of their cell bodies (Galimberti et al., 2010). This topographic specification of TAs appears to involve EphA4, which exhibits a gradient along the dentate gyrus. When EphA4 signaling is disrupted, excessive TAs form at abnormal positions, suggesting that the graded EphA4 suppresses the formation of TAs to establish this synapse map (Galimberti et al., 2010). Therefore, in both the mouse hippocampal and *C. elegans* systems, graded inhibitory cues for synapse formation and maintenance are used to restrict synapse distribution and create synapse topographic maps.

EXPERIMENTAL PROCEDURES

Strains

All strains were maintained as previously described (Brenner, 1974). Transgenic strains were generated by standard injection methods (Mello et al., 1991). The following mutant and transgenic strains were used in this study: *lin-44(n1792)I*, *egl-20(n585)IV*, *lin-17(n671)I*, *mig-1(e1787)I*, *cam-1(gm122)I*, *plx-1(nc36)IV*, *wyIs222(Pmig-13::mcherry::rab-3*, *Punc-4::gfp::rab-3*, *Podr-1::rfp)*, *wyIs320(Pitr-1:plx-1:gfp*, *Pmig-13:mCherry:rab-3*, *Podr-1:gfp)*, *wyEx4271(Pmig-13::mig-1*, *Podr-1::gfp)*, *wyEx5624*, *wyEx5646(Punc-129::lin-17*, *Podr-1::gfp)*, *wyEx5659(Punc-4c::lin-17*, *Podr-1::gfp)*, *wyEx6147 (Plin-44::lin-44*, *Podr-1::gfp)*, *wyEx6150(Pegl-20::lin-44*, *Podr-1::gfp)*, *wyEx6152(Pegl-17::lin-44*, *Podr-1::gfp)*, *wyEx6188(Pmyo-2::lin-44*, *Podr-1::gfp)*, *wyEx3988(Plin-44::egl-20*, *Podr-1::gfp)*, *wyEx6184(Pegl-20::egl-20*, *Podr-1::gfp)*, *wyEx6183 (Pegl-17::egl-20*, *Podr-1::gfp)*, *wyEx6183(Pegl-17::egl-20*, *Podr-1::gfp)*, *wyEx6193(Pitr-1::mig-1::gfp*, *Pmig-13::mCherry::rab-3*, *Podr-1::gfp)*, and *wy6234(Pmig-13::lin-17::mcherry*, *Pmig-13::gfp::rab-3*, *Podr-1::gfp)*.

Fluorescence Microscopy and Confocal Imaging

Images of fluorescently tagged fusion proteins were captured in live *C. elegans* with the use of a Zeiss LSM710 confocal microscope (Carl Zeiss). Worms were immobilized on a 2% agarose pad with 10 mM levamisole (Sigma-Aldrich). Images were analyzed with Zen software (Carl Zeiss).

Plasmid Construction

Expression clones were made in a derivative of pPD49.26 (A. Fire), the pSM vector (a kind gift from S. McCarroll and C.I. Bargmann). *egl-20*, *mig-1*, and *lin-17* cDNAs were amplified from cDNA libraries (Mizumoto and Shen, 2013) with Phusion polymerase (Finnzymes) and gene-specific primer sets. cDNAs were subcloned into *Asc*I/KpnI sites of the pSM. All amplified fragment were sequenced. The *egl-20* primers were 5′-gggGGCGCGCCatgcaatttttca tttgcctg and 3′-gggGGTACCttatttgcatgtatgtactgc. The *mig-1* primers were 5′-ggg GGCGCGCCatgggaccatttcgtggttacc and 3′-ggg GCTAGCccaatcatatt attagttcg. The *lin-17* primers were 5′-gggGGCGCGCCatgatgcattctttgggcatc and 3′-gggGGTACCttagacgaccttactgggtctc.

A 3.9 kb *mig-1* promoter was amplified from N2 genomic DNA and inserted into SphI/AscI sites of the pSM vector. The P*mig-1* primers were 5′-ggg GCATGCatttatgcttctatcccgg and 3′-gggGGCGCGCCtaatgataatggaattgggg.

SUPPLEMENTAL INFORMATION

Supplemental Information includes four figures and can be found with this article online at http://dx.doi.org/10.1016/j.celrep.2013.09.011.

ACKNOWLEDGMENTS

We are grateful to Matthew Klassen and Weizhe Hong for technical assistance and Audrey Howell and Claire Richardson for comments on the manuscript. We thank the Caenorhabditis Genetics Center for strains. This work is supported by the Howard Hughes Medical Institute (to K.S.), National Institutes of Health grant 5R01NS048392 (to K.S.), the Human Frontier Science Program (to K.M.), and the Japan Society for the Promotion of Science (to K.M.).

Received: March 15, 2013
Revised: July 18, 2013
Accepted: September 9, 2013
Published: October 17, 2013

REFERENCES

Brenner, S. (1974). The genetics of *Caenorhabditis elegans*. Genetics *77*, 71–94.

Budnik, V., and Salinas, P.C. (2011). Wnt signaling during synaptic development and plasticity. Curr. Opin. Neurobiol. *21*, 151–159.

Charron, F., and Tessier-Lavigne, M. (2005). Novel brain wiring functions for classical morphogens: a role as graded positional cues in axon guidance. Development *132*, 2251–2262.

Charron, F., and Tessier-Lavigne, M. (2007). The Hedgehog, TGF-beta/BMP and Wnt families of morphogens in axon guidance. Adv. Exp. Med. Biol. *621*, 116–133.

Coudreuse, D.Y., Roël, G., Betist, M.C., Destrée, O., and Korswagen, H.C. (2006). Wnt gradient formation requires retromer function in Wnt-producing cells. Science *312*, 921–924.

Davis, E.K., Zou, Y., and Ghosh, A. (2008). Wnts acting through canonical and noncanonical signaling pathways exert opposite effects on hippocampal synapse formation. Neural Dev. *3*, 32.

Ding, J.B., Oh, W.J., Sabatini, B.L., and Gu, C. (2012). Semaphorin 3E-Plexin-D1 signaling controls pathway-specific synapse formation in the striatum. Nat. Neurosci. *15*, 215–223.

Eisenmann, D.M. (2005). Wnt signaling. WormBook *Jun 25*, 1–17.

Galimberti, I., Bednarek, E., Donato, F., and Caroni, P. (2010). EphA4 signaling in juveniles establishes topographic specificity of structural plasticity in the hippocampus. Neuron *65*, 627–642.

Goldstein, B., Takeshita, H., Mizumoto, K., and Sawa, H. (2006). Wnt signals can function as positional cues in establishing cell polarity. Dev. Cell *10*, 391–396.

Hall, A.C., Lucas, F.R., and Salinas, P.C. (2000). Axonal remodeling and synaptic differentiation in the cerebellum is regulated by WNT-7a signaling. Cell *100*, 525–535.

Harterink, M., and Korswagen, H.C. (2012). Dissecting the Wnt secretion pathway: key questions on the modification and intracellular trafficking of Wnt proteins. Acta Physiol. (Oxf.) *204*, 8–16.

Herman, M.A., Vassilieva, L.L., Horvitz, H.R., Shaw, J.E., and Herman, R.K. (1995). The C. elegans gene lin-44, which controls the polarity of certain asymmetric cell divisions, encodes a Wnt protein and acts cell nonautonomously. Cell *83*, 101–110.

Hilliard, M.A., and Bargmann, C.I. (2006). Wnt signals and frizzled activity orient anterior-posterior axon outgrowth in *C. elegans*. Dev. Cell *10*, 379–390.

Imai, T., Yamazaki, T., Kobayakawa, R., Kobayakawa, K., Abe, T., Suzuki, M., and Sakano, H. (2009). Pre-target axon sorting establishes the neural map topography. Science *325*, 585–590.

Inaki, M., Yoshikawa, S., Thomas, J.B., Aburatani, H., and Nose, A. (2007). Wnt4 is a local repulsive cue that determines synaptic target specificity. Curr. Biol. *17*, 1574–1579.

Kaykas, A., Yang-Snyder, J., Héroux, M., Shah, K.V., Bouvier, M., and Moon, R.T. (2004). Mutant Frizzled 4 associated with vitreoretinopathy traps wild-type Frizzled in the endoplasmic reticulum by oligomerization. Nat. Cell Biol. *6*, 52–58.

Kikuchi, A., Yamamoto, H., and Sato, A. (2009). Selective activation mechanisms of Wnt signaling pathways. Trends Cell Biol. *19*, 119–129.

Kirszenblat, L., Pattabiraman, D., and Hilliard, M.A. (2011). LIN-44/Wnt directs dendrite outgrowth through LIN-17/Frizzled in *C. elegans* Neurons. PLoS Biol. *9*, e1001157.

Klassen, M.P., and Shen, K. (2007). Wnt signaling positions neuromuscular connectivity by inhibiting synapse formation in *C. elegans*. Cell *130*, 704–716.

Komiyama, T., Sweeney, L.B., Schuldiner, O., Garcia, K.C., and Luo, L. (2007). Graded expression of semaphorin-1a cell-autonomously directs dendritic targeting of olfactory projection neurons. Cell *128*, 399–410.

Logan, C.Y., and Nusse, R. (2004). The Wnt signaling pathway in development and disease. Annu. Rev. Cell Dev. Biol. *20*, 781–810.

Luo, L., and Flanagan, J.G. (2007). Development of continuous and discrete neural maps. Neuron *56*, 284–300.

McLaughlin, T., and O'Leary, D.D. (2005). Molecular gradients and development of retinotopic maps. Annu. Rev. Neurosci. *28*, 327–355.

Mello, C.C., Kramer, J.M., Stinchcomb, D., and Ambros, V. (1991). Efficient gene transfer in *C.elegans*: extrachromosomal maintenance and integration of transforming sequences. EMBO J. *10*, 3959–3970.

Mizumoto, K., and Shen, K. (2013). Interaxonal interaction defines tiled presynaptic innervation in *C. elegans*. Neuron *77*, 655–666.

Packard, M., Koo, E.S., Gorczyca, M., Sharpe, J., Cumberledge, S., and Budnik, V. (2002). The *Drosophila* Wnt, wingless, provides an essential signal for pre- and postsynaptic differentiation. Cell *111*, 319–330.

Pan, C.L., Howell, J.E., Clark, S.G., Hilliard, M., Cordes, S., Bargmann, C.I., and Garriga, G. (2006). Multiple Wnts and frizzled receptors regulate anteriorly directed cell and growth cone migrations in *Caenorhabditis elegans*. Dev. Cell *10*, 367–377.

Park, M., and Shen, K. (2012). WNTs in synapse formation and neuronal circuitry. EMBO J. *31*, 2697–2704.

Pecho-Vrieseling, E., Sigrist, M., Yoshida, Y., Jessell, T.M., and Arber, S. (2009). Specificity of sensory-motor connections encoded by Sema3e-Plxnd1 recognition. Nature *459*, 842–846.

Poon, V.Y., Klassen, M.P., and Shen, K. (2008). UNC-6/netrin and its receptor UNC-5 locally exclude presynaptic components from dendrites. Nature *455*, 669–673.

Sato, M., Umetsu, D., Murakami, S., Yasugi, T., and Tabata, T. (2006). DWnt4 regulates the dorsoventral specificity of retinal projections in the *Drosophila melanogaster* visual system. Nat. Neurosci. *9*, 67–75.

Sawa, H. (2012). Control of cell polarity and asymmetric division in *C. elegans*. Curr. Top. Dev. Biol. *101*, 55–76.

Schmitt, A.M., Shi, J., Wolf, A.M., Lu, C.C., King, L.A., and Zou, Y. (2006). Wnt-Ryk signalling mediates medial-lateral retinotectal topographic mapping. Nature *439*, 31–37.

Silhankova, M., and Korswagen, H.C. (2007). Migration of neuronal cells along the anterior-posterior body axis of *C. elegans*: Wnts are in control. Curr. Opin. Genet. Dev. *17*, 320–325.

Sweeney, L.B., Chou, Y.H., Wu, Z., Joo, W., Komiyama, T., Potter, C.J., Kolodkin, A.L., Garcia, K.C., and Luo, L. (2011). Secreted semaphorins from degenerating larval ORN axons direct adult projection neuron dendrite targeting. Neuron *72*, 734–747.

Tran, T.S., Rubio, M.E., Clem, R.L., Johnson, D., Case, L., Tessier-Lavigne, M., Huganir, R.L., Ginty, D.D., and Kolodkin, A.L. (2009). Secreted semaphorins control spine distribution and morphogenesis in the postnatal CNS. Nature *462*, 1065–1069.

Whangbo, J., and Kenyon, C. (1999). A Wnt signaling system that specifies two patterns of cell migration in *C. elegans*. Mol. Cell *4*, 851–858.

White, J.G., Southgate, E., Thomson, J.N., and Brenner, S. (1976). The structure of the ventral nerve cord of *Caenorhabditis elegans*. Philos. Trans. R. Soc. Lond. B Biol. Sci. *275*, 327–348.